Diffuse Traumatic Brain Injury Initially Attenuates and Later Expands Activation of the Rat Somatosensory Whisker Circuit Concomitant with Neuroplastic Responses

Kelley D. Hall[1] and **Jonathan Lifshitz**[1,2,3]

[1]Spinal Cord & Brain Injury Research Center, Chandler Medical Center, University of Kentucky

[2]Department of Anatomy and Neurobiology, Chandler Medical Center, University of Kentucky

[3]Department of Physical Medicine & Rehabilitation, Chandler Medical Center, University of Kentucky

Abstract

Traumatic brain injury can initiate an array of chronic neurological deficits, effecting executive function, language and sensorimotor integration. Mechanical forces produce the diffuse pathology that disrupts neural circuit activation across vulnerable brain regions. The present manuscript explores the hypothesis that the extent of functional activation of brain-injured circuits is a consequence of initial disruption and consequent reorganization. In the rat, enduring sensory sensitivity to whisker stimulation directs regional analysis to the whisker-barrel circuit. Adult, male rats were subjected to midline fluid percussion brain or sham injury and evaluated between 1d and 42d post-injury. Whisker somatosensory regions of the cortex and thalamus maintained cellular composition as visualized by Nissl stain. Within the first week post-injury, quantitatively less *cFos* activation was elicited by whisker stimulation, potentially due to axotomy within and surrounding the whisker circuit as visualized by amyloid precursor protein immunohistochemistry. Over six weeks post-injury, *cFos* activation after whisker stimulation showed a significant linear correlation with time in the cortex (r^2=0.545; p = 0.015), non-significant correlation in the thalamus (r^2=0.326) and U-shaped correlation in the denate gyrus (r^2=0.831), all eventually exceeding sham levels. Ongoing neuroplastic responses in the cortex are evidenced by accumulating growth associated protein and synaptophysin gene expression. In the thalamus, the delayed restoration of plasticity markers may explain the broad distribution of neuronal activation extending into the striatum and hippocampus with whisker stimulation. The sprouting of diffuse-injured circuits into diffuse-injured tissue likely establishes maladaptive circuits responsible for behavioral morbidity. Therapeutic interventions to promote adaptive circuit restructuring may mitigate post-traumatic morbidity.

Keywords

regeneration; ventral posterior media; barrel field; GAP-43; APP; sport-related concussion

Corresponding Author: Jonathan Lifshitz, Ph.D., Spinal Cord & Brain Injury Research Center, University of Kentucky Chandler Medical Center, B463, BBSRB, 741 S. Limestone St., Lexington, KY 40536-0509, Phone: (859) 323-0696, Fax: (859) 257-5737, jlifshitz@uky.edu.

1. Introduction

Annually, 1.5–2.0 million Americans survive a traumatic brain injury (TBI), however 20%–50% of those patients develop persistent functional morbidity within weeks to months after the incident (McAllister, 1992; Langlois et al., 2004). TBI begins with the transient application of a mechanical force to the head (impact or acceleration-deceleration over ~20 msec) that shears cellular membranes, axons and the vasculature (LaPlaca et al., 2007). Following this primary injury, secondary molecular, biochemical and cellular events cause additional neuronal, glial and vascular injuries across multiple brain areas (Thompson et al., 2005; Farkas and Povlishock, 2007). The identification of diffuse axonal injury (DAI) lead to the supposition that neurological dysfunction arises from impaired transport and signaling through injured axons (Povlishock and Stone, 2001; Smith et al., 2003; Povlishock and Katz, 2005; Farkas and Povlishock, 2007; Biasca and Maxwell, 2007). However, axonal injury does not necessarily culminate in neuronal death, rather transient perturbations trend toward recovery over seven days post-injury (Singleton et al., 2002; Singleton and Povlishock, 2004). Cortical, thalamic and hippocampal neurons with peri-somatic axotomy remain viable (Singleton et al., 2002) and do not undergo membrane perturbation (Kelley et al., 2006) or elicit a targeted immune response (Kelley et al., 2007). Furthermore, the early axotomy in the ventral posterior thalamus leads to neuronal atrophy through one week post-injury, which is no longer significant at one month suggesting a reintroduction of trophic support (Lifshitz et al., 2007). This heterogeneous, multi-focal, diffuse brain injury perplexingly spares tissue adjacent to the pathology (Povlishock et al., 1983; Povlishock et al., 1992; Singleton et al., 2002; Singleton and Povlishock, 2004; Kelley et al., 2006; Lifshitz et al., 2007).

Post-traumatic degeneration and synaptic deafferentation are followed by endogenous reparative processes to maintain trophic support and survival (Christman et al., 1997; Emery et al., 2003; Wieloch and Nikolich, 2006). In the diffuse injured brain, damaged tissue would regenerate to and from damaged tissue, typically resulting in circuit reorganization, rather than repair. In contrast, focal injured tissue can be reinnervated by surrounding healthy tissue, which, when successful, provides a substrate for functional recovery (Johansen-Berg, 2007). As a result of uncoordinated regenerative responses (Povlishock and Katz, 2005), diffuse injured circuits could remain disconnected, rewired or intact following the insult. As such, survivors exhibit broad and widespread patterns of neural activation compared to control subjects when functionally imaged during cognitive tasks (Christodoulou et al., 2001; Levine et al., 2002).

By definition, diffuse TBI is more difficult to localize in both the time post-injury and anatomical location than focal TBI. The data in the present manuscript begin to explore the cellular basis for the concurrently observed behavioral sensory sensitivity upon facial whisker stimulation (McNamara et al., 2010). The aberrant behavior provides strict structural landmarks within the somatosensory whisker circuit to examine injury-induced circuit disruption in terms of altered neuronal activation, axonal injury, and synaptic regeneration. By indentifying diffuse injury in a circuit with observable functional deficits, advancements in our understanding of injury-induced mechanisms that result in post-traumatic morbidity can guide therapeutic strategies.

2. Results

With mechanically-induced axotomy and chronic neuronal atrophy in the whisker somatosensory (ventral posterior) thalamus (Kelley et al., 2006; Lifshitz et al., 2007), whisker stimulation evokes aberrant behavioral responses in diffuse brain-injured rats

(McNamara et al., 2010), indicating altered signal processing in a diffuse brain-injured circuit.

2.1 No Overt Histological Damage Evident in the Whisker Barrel Circuit After Diffuse Brain Injury

One set of cytochrome oxidase stained sections were counter-stained with Cresyl Violet to demonstrate that cortical barrels and thalamic barreloids do not sustain focal damage after diffuse injury (Figure 2). Individual cortical barrels remain well defined by cytochrome oxidase histochemistry and filled with nissl-positive cells in sham and diffuse-injured brains. No apparent injury-related change in barrel architecture or cellular profile is evident over the post-injury period. Arbitrarily angled sections are required to capture discrete thalamic barreloids in the ventral posterior medial thalamus (Haidarliu and Ahissar, 2001). In coronal sections, similar histochemical and histological staining are evident in sham and diffuse-injured brains. No gross changes in cellular composition or distribution are evident, supporting previous reports of an absence of neuronal loss (Lifshitz et al., 2007).

2.2 Whisker Stimulation Induces Widespread Neuronal Activation

The holistic changes in the physical and affective perception of whisker stimulation in brain-injured rodents suggest that circuits beyond the somatosensory whisker-barrel pathway become activated upon whisker stimulation (McNamara et al., 2010). Before transcardial perfusion, all but two whiskers per side were clipped and then stimulated for 30 min to activate neuronal circuits responsive to whisker stimulation as identified by immediate early gene *cFos* immunohistochemistry. Over the observed time course, whisker stimulation activated neurons in the cortical barrels in layer IV of primary sensory cortex (Figure 3A–C) and thalamic barreloids in the ventral posterior medial thalamus (Figure 3D–F) in sham and brain-injured animals. By 28 days and through 42 days post-injury, stimulation-induced *cFos* activation was observed in area CA3 (Figure $3H_1$, $3I_1$) and the hilus (Figure $3H_3$, $3I_3$) of the hippocampus in contrast to the absence of activated neurons in uninjured sham brain (Figure $3G_1$, $3G_3$). Area CA1 of the hippocampus showed immunoreactivity that did not appear to depend on injury group (Figure $3G_2$, $3H_2$, $3I_2$). In the striatum (Figure 3J–L), stimulation resulted in *cFos* activation that was restricted to the dorsal striatum (Figure $3J_1$) in sham animals, but both the dorsal (Figure $3K_1$, $3L_1$) and ventral striatum (Figure $3K_2$, $3L_2$) in injured brain. Neuronal activation in the posterior medial nucleus of the thalamus (PoMN, Figure 3M–O), an efferent nucleus for whisker movement (Waite and Tracey, 1995), did not demonstrate injury-related differences, despite feedback control in the sensorimotor circuit. Neuronal activation, if any, in other brain regions, including the amygdala and posterior nucleus, was not different between injured and uninjured animals (data not shown). Based on regional localization and cellular morphology, the *cFos* immunoreactivity was restricted to gray matter and particularly neurons. Therefore, the long-term consequences of diffuse brain injury include widespread circuit activation in response to specific sensory input.

2.3 Sensory Activation of the Diffuse-Injured Brain is Initially Attenuated and Later Augmented

The somatosensory cortical barrels, ventral posterior thalamus and hippocampus maintain strict structural landmarks that can be used to guide quantitative analysis. Histological staining was quantified based on the percentage of digital image pixels exceeding a threshold level of staining. This procedure is exclusive of staining intensity and rather focuses on the relative extent of staining, expressed as a percent of all pixels in defined regions of interest.

For the primary somatosensory cortical barrel field, data from uninjured sham animals indicate 4.3 ±0.8% of the defined cortical barrels show *cFos*-positive staining in response to whisker stimulation (Figure 4A). Between one and seven days post-injury, the relative *cFos* activation was less than sham, and then increased above sham levels by 42 days post-injury. The significant linear correlation between *cFos* labeling and days post-injury (r^2=0.545; $F(1,8) = 9.58$; $p = 0.015$) bridges the sham value near three weeks post-injury.

For the ventral posterior thalamus, data from uninjured sham animals indicate 2.4 ±0.6% of the defined dorsal regions show *cFos*-positive staining in response to whisker stimulation (Figure 4B). Between one and seven days post-injury, the relative *cFos* activation was less than or equal to sham, and then returned to sham levels by 42 days post-injury. The linear regression between cFos labeling and days post-injury (r^2=0.326; $F(1,9) = 4.35$; $p = 0.067$) bridges the sham value near three weeks post-injury.

For the hippocampus, data from uninjured sham animals indicate 3.7 ±0.7% and 3.6 ±0.3% of the dentate gyrus and area CA3, respectively, show *cFos*-positive staining in response to whisker stimulation (Figure 4C, 4D). For the dentate gyrus, *cFos* activation in brain-injured animals remains within sham values for the first two days and then attenuates over seven through 28 days. Values exceeded sham values by 42 days post-injury, resulting in a U-shaped relationship between activation and time post-injury (r^2=0.831; $y = 0.0001x^2 - 0.0041x + 0.0474$). For area CA3, *cFos* activation does not appear to change significantly from sham values over time post-injury (r^2=0.036; $F(1,8) = 0.299$; $p = 0.599$).

The initial hypo-activation followed by chronic hyper-activation in discrete loci indicates an initial circuit disruption and a delayed recovery from diffuse brain injury.

2.4 Traumatic Axonal Injury: An Initiating Mechanism for Circuit Disruption

The anterograde transported amyloid precursor protein (APP) accumulates at sites of cytoskeletal damage to indicate axonal injury and axotomy associated with the initiating mechanical forces of TBI (Kelley et al., 2006). In comparison to the absence of staining in sham brain (Figure 5A), multi-focal sites of traumatic axonal injury can be identified by immunocytochemistry at 1–2 days post-injury that include the subcortical white matter (Figure 5B), superior thalamic radiation (Figure 5C), internal capsule (Figure 5D) and fimbria of the hippocampus (Figure 5E). Moreover, axotomy was confirmed in grey matter regions (data not shown), as previously reported (Kelley et al., 2006; Lifshitz et al., 2007). Traumatic axonal injury is concomitant with petechial hemorrhage, shown in the subcortical white matter (Figure 5B) and fimbria of the hippocampus (Figure 5E). However, the traumatic axonal injury does not uniformly effect all neurons within a given loci, resulting in a heterogeneous pathology (Singleton and Povlishock, 2004).

2.5 Neuroplasticity Gene Expression Supports Injury-Induced Circuit Rewiring

A series of robust, but unregulated, neuroplastic events may be initiated in response to the traumatic axotomy sustained by a fraction of the neuronal population in order to maintain cellular viability (Lifshitz et al., 2007). In an initial attempt to identify a neuroplastic, regenerative response after diffuse brain injury, sets of tissue were immunostained for growth-associated protein 43 (GAP-43), a pre-synaptic regenerative marker (Hulsebosch et al., 1998) or synaptophysin, a marker of synaptic reorganization (Bergmann et al., 1997). In experimental brain injury, GAP-43 and synaptophysin have been reported as markers of regenerative sprouting (Christman et al., 1997; Hulsebosch et al., 1998; Emery et al., 2000; Thompson et al., 2006). In the chronic, diffuse-injured brain distinguishing regenerated circuits from uninjured, intact circuits remains inconclusive. High background levels of these ubiquitous proteins were not appreciably altered in the diffuse-injured brain

(Supplementary Figure 1), affirming immunohistochemistry approaches as insensitive to detect coordinated regenerative responses.

Quantitative real-time polymerase chain reaction (qPCR) was used to determine relative levels of injury-induced change in gene expression related to sprouting. At 7 days and 28 days after brain injury, GAP-43 and synaptophysin gene expression was quantified in the somatosensory whisker cortex (S1BF), thalamus (VPM) and hippocampus relative to uninjured sham (Figure 6). In the primary somatosensory barrel cortex (S1BF; Figure 6, *left*), GAP-43 expression trended towards an increase over time post-injury ($F(2,8)=3.50$; $p=0.081$), outpacing the expression of synaptophysin ($F(2,8)=0.95$; $p=0.427$), but neither achieved significance. In the ventral posterior medial thalamus (VPM; Figure 6, *middle*), diffuse brain injury resulted in significantly reduced gene expression of GAP-43 ($F(2,7)=5.80$; $p=0.033$) and synaptophysin ($F(2,8)=6.07$; $p=0.025$) at 7 days post-injury, which recovered to sham levels by 28 days post-injury. In the whole hippocampus (Figure 6, *right*), gene expression for GAP-43 ($F(2,8)=5.56$; $p=0.031$) and synaptophysin ($F(2,8)=14.17$; $p=0.002$) mirrored the results for the thalamus and significantly exceeded sham levels at 28 days post-injury. Therefore, neuroplastic responses are evident within the thalamic relay of the whisker barrel circuit and extend into the hippocampus following diffuse brain injury in the rat, which may not necessarily provide complete circuit restoration.

3. Discussion

In the diffuse brain-injured rat, whisker stimulation elicits behavioral morbidity (McNamara et al., 2010) and altered patterns of neuronal activation (Figure 3) at one month post-injury, without overt destruction of the somatosensory whisker circuit (Figure 2). Traumatic axonal injury initiated by the primary injury (Figure 5) could be the precipitating anatomical event that disconnects some thalamocortical projection neurons from their cortical targets, without cell death (Singleton et al., 2002; Lifshitz et al., 2007). The surviving neurons display atrophic change at one day and one week post-injury (Lifshitz et al., 2007), reflecting a loss of trophic support. In response to injury, collateral sprouting of injured axons throughout the brain may ensure neuronal survival, despite the functional neurological consequences of circuit reorganization. By one month post-injury, the atrophy is no longer significant suggesting a restoration of neurotrophic support (Franklin and Johnson, 1998; Lifshitz et al., 2007). In the adult central nervous system, sprouting would not be capable of reconnecting the disconnected projection circuits; rather maladaptive local connections are more likely to be established. Inappropriate connections within and between local domains would disrupt neural signaling, aberrant signals would become amplified in ascending systems, and likely manifest in behavioral morbidity (Jones and Pons, 1998). Simply, the axotomized projection neurons that survive would function as interneurons, scattering neural information.

Experimental, diffuse TBI does not result in overt cavitation, hematoma or edema (Farkas and Povlishock, 2007; McGinn et al., 2009). In fact, the thalamic relay and cortical domains for whisker somatosensation remain unremarkable post-injury. At the cellular level, whisker stimulation activates the predicted thalamic and cortical domains, but also recruits additional brain regions in the chronic injured brain. At one month post-injury, *cFos* was observed in the ventral striatum and hippocampal area CA3, in contrast to uninjured brains. Over six weeks post-injury, *cFos* activation after whisker stimulation showed significant correlations with time, eventually returning to or exceeding sham levels. The quantification method employed is based on immuno-positive pixels, rather than the number of immuno-positive neurons. Neuronal atrophy could contribute to the early reductions in *cFos* activation, whereas the delayed increases in activation are unlikely to be associated with hypertrophy. Similarly, the contusion associated with the mixed focal and diffuse model of para-sagittal

fluid percussion impairs the predicted metabolic activation of cortical and thalamic domains with whisker stimulation acutely and through two months post-injury (Dietrich et al., 1994; Passineau et al., 2000). Regardless, the simultaneous time courses for the sprouting response and circuit activation (initial attenuation followed by expansion) indicate a cellular response to brain injury for the restoration of circuit function after diffuse brain injury.

3.1 Initiating Mechanism for Circuit Disruption and Reactive Sprouting

Multifocal sites of axonal injury were evident acutely after brain injury, notably in the superior thalamic radiation, internal capsule, subcortical white matter and fimbria of the hippocampus. The mechanical forces of the injury sever axons apparently indiscriminately, leaving a fraction of the neurons with an axotomy in the peri-somatic domain that does not result in neuronal death (Singleton et al., 2002; Kelley et al., 2006; Lifshitz et al., 2007). During this acute axotomy period, whisker stimulation is less likely to activate neurons.

The delayed onset behavioral morbidity suggests that endogenous repair of the injured brain is either incomplete or incorrect. Diffuse brain injury initiates regional specific neuroplastic responses (GAP-43 and synaptophysin gene expression) in the somatosensory whisker circuit, suggesting persistent dynamic circuit reorganization within the timeframe of aberrant behavioral responses to whisker stimulation. In the cortex, plasticity markers continually increased, whereas plasticity markers in the thalamus and hippocampus initially decreased and then returned to uninjured levels. Immunohistochemically, GAP-43 protein expression in the cortex and hippocampus have been reported to peak and subside within a week after midline fluid percussion (Hulsebosch et al., 1998). These regional differences may represent regional susceptibility to diffuse injury and inherent heterogeneity of neuroplastic responses to brain injury. In focal brain injury, synaptophysin protein expression followed GAP-43 expression, suggesting that sprouting may precede synaptogenesis (Thompson et al., 2006). Also, axotomy without cell loss is sufficient to induce a regenerative response, as neurons axotomized close to the cell body demonstrate increased GAP-43 levels (Doster et al., 1991). Similarly, *in vivo* axotomy of layer V pyramidal neurons and a cortical stab lesion upregulate GAP-43 expression without cell loss (Darian-Smith and Gilbert, 1994; Vaudano et al., 1995; Di et al., 2005). The regenerative potential of the whisker circuit is exhibited by the rapid rearrangement of cortical barrel representations when whiskers are stimulated or removed (Dunn-Meynell et al., 1992; Feldman and Brecht, 2005). Whether injury-induced sprouting accumulates as in the cortex or rebounds as in the thalamus, only a small fraction of misconnected neurons would be necessary to interfere with corticothalamic and thalamocortical circuit function, as demonstrated by *cFos* activation.

Injury-induced remodeling could be an exploitation of inherent structural plasticity (local changes in synaptic strength and connectivity) (Chklovskii et al., 2004; Debello, 2008; Holtmaat et al., 2008). Studies in disparate fields of cognition, sensory plasticity and peripheral nerve injury have shown that remodeling in the adult brain occurs over several millimeters through the growth of axonal and dendritic branches to form novel connections over prolonged time periods (Pons et al., 1991; Jones, 2000; Dancause et al., 2005; Jain et al., 2008). Under normal circumstances or in response to focal injury, these neuroplastic responses may enhance circuit function. After diffuse brain injury, the capacity of the brain to rewire could be commandeered to take advantage of silent synapses and create new synapses, which allows individual neurons to recover and survive despite the consequences on circuit function. The absence of atrophic change at one month post-injury suggests a reintroduction of trophic support (Franklin and Johnson, 1998; Lifshitz et al., 2007). No significant net changes in neuron or synapse number would necessarily need to occur for behavioral morbidity to emerge after injury.

Denervated post-synaptic sites likely also survive the loss of presynaptic inputs and initiate neuroplastic responses that partially or fully reinnervate those sites (Povlishock et al., 1992). Similarly, regenerative sprouting could occur in undamaged axons to further disrupt circuit function and influence behavioral morbidity. Behavioral morbidities may emerge as a consequence of global activation and an inability to discern useful information from elevated background noise, as has been demonstrated in sensory integration disorder, a component of Autism Spectrum Disorder (Iarocci and McDonald, 2006). Aberrant sprouting also has been suggested to contribute to post-traumatic epilepsy, recovery from cortical stroke and the neuronal changes in Alzheimer's disease (Carmichael, 2003; Chuckowree et al., 2004). Regardless, the formation of new synapses and therefore new circuits may be responsible for functional deficits associated with neurological disease.

3.2 Repair Differs Between Focal and Diffuse Brain Injured Circuits

Focal injury induces reinnervation of damaged tissue by surrounding healthy tissue and, when successful, provides a substrate for functional recovery (Johansen-Berg, 2007). Years after upper limb deafferentation in the monkey, thalamic and cortical neurons undergo transneuronal atrophy, with remarkably little cell loss and considerable evidence for circuit reorganization (Jones, 2000). Similarly, cortical ischemia creates a favorable environment that permits long-range sprouting from perilesional and distal cortical regions (Dancause et al., 2005; Carmichael et al., 2005). Similar, but different, diffuse injury induces a regenerative response (frank regeneration, collateral sprouting, or synaptic plasticity) within damaged tissue towards adjacent damaged tissue that would typically result in circuit reorganization. In the absence of glial scaring or a necrotic focus, regenerative responses are not guided towards an injury focus, but rather occur locally between diffuse-injured regions in an unregulated manner. Transneuronal atrophy and delayed recovery is evident by the transient reduction of neuronal nuclear volume in the somatosensory thalamus after diffuse brain injury (Lifshitz et al., 2007). Moreover, reorganization in a relatively small volume in subcortical tissue would diverge significantly at the cortical level to amplify the structural alterations (Jones and Pons, 1998). Morbidity may also arise from similar neuroplastic events occurring within the descending cortical pathways. The injury-induced structural alterations are likely to be permanent in the absence of therapeutic interventions, forming the organic basis for persistent behavioral morbidity. The abrupt and extensive circuit reorganization initiated by diffuse brain injury may further deplete the capacity for adaptive change to subsequent challenges (Kolb et al., 1998), thereby contributing to enduring post-traumatic morbidity.

3.3 Conclusion

The present manuscript addresses the cellular basis of circuit reorganization underlying a previously reported diffuse brain injury-induced behavioral morbidity (McNamara et al., 2010). The anatomical guideposts of the whisker barrel circuit direct functional, anatomical and molecular analyses of experimental diffuse brain injury in order to evaluate post-traumatic morbidity. Cellular signaling in the injured brain likely favors axonal growth and survival, with the adverse outcome of maladaptive plasticity. The appropriate pharmacological treatment in concert with relevant physical therapy (whisker stimulation) may enhance adaptive restructuring and promote functional recovery. These studies provide a model to explore the causes of persistent morbidity experienced by survivors of mild to moderate TBI, for whom treatment options are limited.

4. Experimental Procedure

4.1 Midline Fluid Percussion Brain Injury

Adult male Sprague–Dawley rats (375–400 g; n = 27) were subjected to midline fluid percussion injury (FPI) consistent with methods described previously (Lifshitz et al., 2007; Lifshitz, 2008). Briefly, rats were anesthetized with 4% isoflurane in 70% N_2O and 30% O_2, intubated, and maintained on a ventilator with 2% isoflurane. During surgery, body temperature was maintained at 37°C with a thermostat controlled heating pad (Harvard Apparatus, Holliston, MA). In a head holder assembly (Kopf Instrument, Tujunga, CA), a midline scalp incision exposed the skull. A 4.8-mm circular craniotomy was performed (centered on the sagittal suture midway between bregma and lambda) without disrupting the underlying dura or superior sagittal sinus. An injury cap was fabricated from the female portion of a Leur-Loc needle hub, which was cut, beveled, and scored to fit within the craniotomy. Skull screws were secured in 1-mm holes hand-drilled into the right frontal and occipital bones. The injury hub was affixed over the craniotomy using cyanoacrylate gel and methyl-methacrylate (Hygenic Corp., Akron, OH) was applied around the injury hub and screws. The scalp was sutured closed over the hub, topical Lidocaine ointment was applied, and the animal was extubated. Animals were returned to a warmed holding cage and monitored until ambulatory (approximately 60–90 min). Additional animals included in the gene expression studies were treated similarly, except that isoflurane was delivered in 100% O_2 via nosecone.

For injury induction, animals were re-anesthetized with 4% isoflurane. The incision was opened and the injury hub was filled with normal saline and attached to the male end of the fluid percussion device (Custom Design and Fabrication, Virginia Commonwealth University, Richmond, VA). An injury of moderate severity (1.9–2.0 Atm; n = 19) was administered by releasing the pendulum onto the fluid-filled piston (Dixon et al., 1987; Lifshitz, 2008), as reflexive responses returned. After injury, the injury hub assembly was removed *en bloc*, bleeding was controlled with Gelfoam (Pharmacia, Kalamazoo, MI), and the incision was sutured. Animals were monitored for spontaneous respiration and the return of the righting reflex. After recovery of the righting reflex, animals were placed in a warmed holding cage before being returned to the vivarium. For sham-injured animals (n = 8), the identical surgical procedures were followed, without the induction of the injury, and distributed across post-injury time points. Righting reflex times greater than 6 minutes in all brain-injured animals indicated a moderate injury severity, compared to less than 15 seconds for sham-injured animals. Experiments were conducted in accordance with NIH and institutional guidelines concerning the care and use of laboratory animals (IACUC). Adequate measures were taken to minimize pain or discomfort.

4.2 Tissue preparation and Cytochrome Oxidase Histochemistry

At 1 day, 7 days, 28 days or 42 days after moderate midline fluid percussion brain or sham injury (n = 2–4/group), rats were briefly anesthetized with inhaled isoflurane and all but two of the posterior macrovibrissae per side were clipped using surgical scissors. After a 60 minute recovery, the remaining whiskers were manually stimulated for 30 min before transcardial perfusion. Animals were euthanized by an overdose of sodium pentobarbital (150 mg/kg, i.p.) and transcardially perfused with 4% paraformaldehyde/0.1% glutaraldehyde in Millonig's buffer for immunocytochemistry. Brains were removed, blocked in the coronal plane and sectioned in 0.1 M phosphate buffer (PBS) at a thickness of 40 µm using a vibratome (Leica Microsystems, Bannockburn, IL). As much as reasonably possible, the brains and tissue sections were protected from light during and following the sectioning. Twelve sets of serial coronal sections were collected in 0.1 M PBS (480 µm between sections in a given set). Immediately following the tissue sectioning, all sections

were reacted for cytochrome oxidase histochemistry. The PBS was replaced with syringe-filtered (0.2 μm) staining solution (4% sucrose, 0.05% diaminobenzidine, 0.05% cytochrome c [type IV, Sigma-Aldrich C7752] in PBS). Sections were incubated in an oven at 37 °C on an orbital shaker in the dark for 2–3 hours. After the first hour, the staining solution was replaced with fresh solution. Sections were checked for reddish-brown staining intensity every 30 minutes. The histochemical reaction was stopped with three rinses of 4°C PBS for 10 minutes each. Sections were stored at 4°C in PBS until immunohistochemical or Cresyl Violet staining.

4.3 Immunohistochemistry

Separate sets of tissue from each animal were immuno-stained for the immediate early gene *cFos*, amyloid precursor protein (APP), presynaptic growth associated protein 43 (GAP-43) or synaptophysin. Sections were subjected to microwave antigen retrieval in citric acid and visualized with nickel-enhanced diaminobenzidine to discriminate antigen stain from cytochrome oxidase histochemistry, as modified from previous methods (Stone et al., 1999; Kelley et al., 2006; Kelley et al., 2007). Briefly, endogenous peroxidase activity was quenched with 0.3% H_2O_2 in PBS for 30 min. After antigen retrieval in citric acid, sections were pre-incubated in 10% normal goat serum (NGS) with 0.2% Triton X-100 in PBS (60 min), and incubated overnight with a primary antibody in 1% NGS in PBS. Primary antibodies include *cFos* (1:4000, sc-52, rabbit anti-*cFos*, Santa-Cruz Biotech), APP (1:1500, rabbit anti-C-terminus specific APP, Invitrogen), GAP-43 (1:2000, mouse anti-GAP-43, Sigma) and synaptophysin (1:2000, rabbit anti-synaptophysin, Invitrogen). Then, sections were incubated (60 min) in biotinylated goat anti-rabbit (1:200) or mouse (1:1000) IgG secondary antibody (Vector Labs) in 1% NGS in PBS. Immunostaining was visualized using avidin:biotinylated enzyme complex (Vectastain ABC Standard Elite Kit; Vector) for 1h followed by 0.015% diaminobenzidine, 0.4% nickel sulfate, and 0.006% H_2O_2 in 0.1M phosphate buffer for 10–20 min. Sections were dehydrated and coverslipped. Additional sections processed without primary antibody served as a control. Images were captured using an Olympus AX80 microscope equipped with an integrated digital camera and image capture software. Final publication micrographs were adjusted to utilize the maximum range of levels in the red, green and blue channels (Adobe Photoshop CS2).

4.4 Quantification of Neuronal Activation

Primary quantification of the *cFos* reaction product in the cortical barrels, ventral posterior thalamus and hippocampus was conducted by calculating the percentage of immuno-positive pixels within strict structural landmarks from digital photomicrographs, comparable to the gray-level-index as previously described (Bisler et al., 2002). Briefly, regions of interest were traced onto grayscale images of immuno-positive staining, using cytochrome oxidase histochemistry to highlight regional boundaries. The barrels of primary somatosensory cortex bordered on cortical layer I, the inter-barrel septa and cortical layer VI (Figure 1). The ventral posterior nucleus of the thalamus bordered on the reticular nucleus, superior thalamic radiation and the posterior nucleus, limited ventrally through its midsection. The dentate gyrus bordered on the molecular layer and the linear segment to the end of CA4. Area CA3 of the hippocampus bordered on the linear segments from the dentate gyrus to CA4 and included the alveus to stratum moleculare. The grayscale pixel distribution was digitally thresholded to separate positive stained pixels from unstained pixels (BioQuant, BioQuant Image Analysis Corporation). The thresholded image was then segmented into white and black pixels, indicating positive and negative staining, respectively (Figure 1). Two or three sections per animal containing the regions of interest were quantified in triplicate to calculate the *cFos* labeling as percent of *cFos* positive pixels (white pixels) in the region of interest (white + black pixels). The change in regional activation with reference to the mean sham value was evaluated as a function of days post-injury by regression

analysis to indicate the rate and phases of circuit activation influenced by diffuse brain injury

4.5 Real-Time Quantitative PCR

Twelve additional animals were generated for quantitative real-time polymerase chain reaction (qPCR), which has the sensitivity to detect the expression of low abundance mRNA transcripts in small tissue samples of individual animals. Sham (n = 4), 7 day (n = 4) and 28 day (n = 4) brain-injured rats were perfused with cold saline, and tissue samples from primary somatosensory barrel cortex (S1BF), ventral posterior medial thalamus (VPM) and the whole hippocampus were obtained by dissection from 2 mm coronal sections. mRNA content was stabilized (RNAlater, Qiagen Corp) and stored frozen. Isolated mRNA (RNeasy, Qiagen Corp) was quantified (NanoDrop ND-1000 spectrophotometer), converted to complementary DNA (cDNA; High Capacity cDNA Archive Kit, Applied Biosystems Inc.) and then used as a template (200 ng based on original RNA concentrations) for commercially-available gene expression assays, according to manufacturer's protocols. To evaluate the injury-related neuroplastic response, two sprouting-related genes, GAP-43 (Rn00567901_m1) and synaptophysin (Rn00561986_m1), were quantified in triplicate (StepONE, Applied Biosystems) according to manufacturer's protocols. The Applied Biosystems TaqMan® Gene Expression Assays are optimized to run under universal thermal cycling conditions, with amplification efficiencies of 100%. Within each animal, relative gene expression was normalized to the 18s rRNA endogenous control (part number 4352930E) and the average threshold cycle in the sham group using the $2^{-\Delta\Delta CT}$ method (Livak and Schmittgen, 2001), which relates gene expression to the PCR cycle number at which the fluorescence signals exceed a threshold above baseline. Relative gene expression was analyzed by one-way ANOVA and a Newman-Keuls post-test, with significance set at $p<0.05$.

Supplementary Material

Refer to Web version on PubMed Central for supplementary material.

Abbreviations

APP	Amyloid precursor protein
CA	Cornu ammonis of the hippocampus
cDNA	Complementary DNA
DAI	Diffuse axonal injury
FPI	Fluid percussion injury
GAP-43	Growth-associated protein 43 kDa
IACUC	Institutional animal care and use committee
NGS	Normal goat serum
PBS	Phosphate buffered saline
PoMN	Posterior medial nucleus of the thalamus
qPCR	Quantitative real-time polymerase chain reaction
S1BF	Primary somatosensory barrel field
TBI	Traumatic brain injury

VPM   Ventral posterior medial nucleus of the thalamus

Acknowledgments

References

Bergmann M, Post A, Rittel I, Bechmann I, Nitsch R. Expression of synaptophysin in sprouting neurons after entorhinal lesion in the rat. Exp Brain Res. 1997; 117:80–86. [PubMed: 9386006]

Biasca N, Maxwell WL. Minor traumatic brain injury in sports: a review in order to prevent neurological sequelae. Prog Brain Res. 2007; 161:263–291. [PubMed: 17618984]

Bisler S, Schleicher A, Gass P, Stehle JH, Zilles K, Staiger JF. Expression of c-Fos, ICER, Krox-24 and JunB in the whisker-to-barrel pathway of rats: time course of induction upon whisker stimulation by tactile exploration of an enriched environment. J Chem Neuroanat. 2002; 23:187–198. [PubMed: 11861125]

Carmichael ST. Plasticity of cortical projections after stroke. Neuroscientist. 2003; 9:64–75. [PubMed: 12580341]

Carmichael ST, Archibeque I, Luke L, Nolan T, Momiy J, Li S. Growth-associated gene expression after stroke: evidence for a growth-promoting region in peri-infarct cortex. Exp Neurol. 2005; 193:291–311. [PubMed: 15869933]

Chklovskii DB, Mel BW, Svoboda K. Cortical rewiring and information storage. Nature. 2004; 431:782–788. [PubMed: 15483599]

Christman CW, Salvant JB Jr, Walker SA, Povlishock JT. Characterization of a prolonged regenerative attempt by diffusely injured axons following traumatic brain injury in adult cat: a light and electron microscopic immunocytochemical study. Acta Neuropathol (Berl). 1997; 94:329–337. [PubMed: 9341933]

Christodoulou C, DeLuca J, Ricker JH, Madigan NK, Bly BM, Lange G, Kalnin AJ, Liu WC, Steffener J, Diamond BJ, Ni AC. Functional magnetic resonance imaging of working memory impairment after traumatic brain injury. J Neurol Neurosurg Psychiatry. 2001; 71:161–168. [PubMed: 11459886]

Chuckowree JA, Dickson TC, Vickers JC. Intrinsic regenerative ability of mature CNS neurons. Neuroscientist. 2004; 10:280–285. [PubMed: 15271255]

Dancause N, Barbay S, Frost SB, Plautz EJ, Chen D, Zoubina EV, Stowe AM, Nudo RJ. Extensive cortical rewiring after brain injury. J Neurosci. 2005; 25:10167–10179. [PubMed: 16267224]

Darian-Smith C, Gilbert CD. Axonal sprouting accompanies functional reorganization in adult cat striate cortex. Nature. 1994; 368:737–740. [PubMed: 8152484]

Debello WM. Micro-rewiring as a substrate for learning. Trends Neurosci. 2008; 31:577–584. [PubMed: 18817991]

Di GS, Faden AI, Yakovlev A, Duke-Cohan JS, Finn T, Thouin M, Knoblach S, De BA, Bregman BS, Hoffman EP. Neuronal plasticity after spinal cord injury: identification of a gene cluster driving neurite outgrowth. FASEB J. 2005; 19:153–154. [PubMed: 15522907]

Dietrich WD, Alonso O, Busto R, Ginsberg MD. Widespread metabolic depression and reduced somatosensory circuit activation following traumatic brain injury in rats. J Neurotrauma. 1994; 11:629–640. [PubMed: 7723063]

Dixon CE, Lyeth BG, Povlishock JT, Findling RL, Hamm RJ, Marmarou A, Young HF, Hayes RL. A fluid percussion model of experimental brain injury in the rat. J Neurosurg. 1987; 67:110–119. [PubMed: 3598659]

Doster SK, Lozano AM, Aguayo AJ, Willard MB. Expression of the growth-associated protein GAP-43 in adult rat retinal ganglion cells following axon injury. Neuron. 1991; 6:635–647. [PubMed: 1826603]

Dunn-Meynell AA, Benowitz LI, Levin BE. Vibrissectomy induced changes in GAP-43 immunoreactivity in the adult rat barrel cortex. J Comp Neurol. 1992; 315:160–170. [PubMed: 1531989]

Emery DL, Raghupathi R, Saatman KE, Fischer I, Grady MS, McIntosh TK. Bilateral growth-related protein expression suggests a transient increase in regenerative potential following brain trauma. J Comp Neurol. 2000; 424:521–531. [PubMed: 10906717]

Emery DL, Royo NC, Fischer I, Saatman KE, McIntosh TK. Plasticity following injury to the adult central nervous system: is recapitulation of a developmental state worth promoting? J Neurotrauma. 2003; 20:1271–1292. [PubMed: 14748977]

Farkas O, Povlishock JT. Cellular and subcellular change evoked by diffuse traumatic brain injury: a complex web of change extending far beyond focal damage. Prog Brain Res. 2007; 161:43–59. [PubMed: 17618969]

Feldman DE, Brecht M. Map plasticity in somatosensory cortex. Science. 2005; 310:810–815. [PubMed: 16272113]

Franklin JL, Johnson EM. Control of neuronal size homeostasis by trophic factor-mediated coupling of protein degradation to protein synthesis. J Cell Biol. 1998; 142:1313–1324. [PubMed: 9732291]

Haidarliu S, Ahissar E. Size gradients of barreloids in the rat thalamus. J Comp Neurol. 2001; 429:372–387. [PubMed: 11116226]

Holtmaat A, De PV, Wilbrecht L, Knott GW. Imaging of experience-dependent structural plasticity in the mouse neocortex in vivo. Behav Brain Res. 2008; 192:20–25. [PubMed: 18501438]

Hulsebosch CE, DeWitt DS, Jenkins LW, Prough DS. Traumatic brain injury in rats results in increased expression of Gap-43 that correlates with behavioral recovery. Neurosci Lett. 1998; 255:83–86. [PubMed: 9835220]

Iarocci G, McDonald J. Sensory integration and the perceptual experience of persons with autism. J Autism Dev Disord. 2006; 36:77–90. [PubMed: 16395537]

Jain N, Qi HX, Collins CE, Kaas JH. Large-scale reorganization in the somatosensory cortex and thalamus after sensory loss in macaque monkeys. J Neurosci. 2008; 28:11042–11060. [PubMed: 18945912]

Johansen-Berg H. Structural plasticity: rewiring the brain. Curr Biol. 2007; 17:R141–R144. [PubMed: 17307051]

Jones EG. Cortical and subcortical contributions to activity-dependent plasticity in primate somatosensory cortex. Annu Rev Neurosci. 2000; 23:1–37. [PubMed: 10845057]

Jones EG, Pons TP. Thalamic and brainstem contributions to large-scale plasticity of primate somatosensory cortex. Science. 1998; 282:1121–1125. [PubMed: 9804550]

Kelley BJ, Farkas O, Lifshitz J, Povlishock JT. Traumatic axonal injury in the perisomatic domain triggers ultrarapid secondary axotomy and Wallerian degeneration. Exp Neurol. 2006; 198:350–360. [PubMed: 16448652]

Kelley BJ, Lifshitz J, Povlishock JT. Neuroinflammatory responses after experimental diffuse traumatic brain injury. J Neuropathol Exp Neurol. 2007; 66:989–1001. [PubMed: 17984681]

Kolb B, Forgie M, Gibb R, Gorny G, Rowntree S. Age, experience and the changing brain. Neurosci Biobehav Rev. 1998; 22:143–159. [PubMed: 9579307]

Langlois, JA.; Rutland-Brown, W.; Thomas, KE. Traumatic brain injury in the United States: emergency department visits, hospitalizations, and deaths. Atlanta, GA: Centers for Disease Control and Prevention, National Center for Injury Prevention and Control; 2004.

LaPlaca MC, Simon CM, Prado GR, Cullen DK. CNS injury biomechanics and experimental models. Prog Brain Res. 2007; 161:13–26. [PubMed: 17618967]

Levine B, Cabeza R, McIntosh AR, Black SE, Grady CL, Stuss DT. Functional reorganisation of memory after traumatic brain injury: a study with H(2)(15)0 positron emission tomography. J Neurol Neurosurg Psychiatry. 2002; 73:173–181. [PubMed: 12122177]

Lifshitz, J. Fluid Percussion Injury. In: Chen, J.; Xu, Z.; Xu, X-M.; Zhang, J., editors. Animal Models of Acute Neurological Injuries. Totowa, NJ: The Humana Press, Inc.; 2008.

Lifshitz J, Kelley BJ, Povlishock JT. Perisomatic thalamic axotomy after diffuse traumatic brain injury is associated with atrophy rather than cell death. J Neuropathol Exp Neurol. 2007; 66:218–229. [PubMed: 17356383]

Livak KJ, Schmittgen TD. Analysis of relative gene expression data using real-time quantitative PCR and the 2(−Delta Delta C(T)) Method. Methods. 2001; 25:402–408. [PubMed: 11846609]

McAllister TW. Neuropsychiatric sequelae of head injuries. Psychiatr Clin North Am. 1992; 15:395–413. [PubMed: 1603732]

McGinn MJ, Kelley BJ, Akinyi L, Oli MW, Liu MC, Hayes RL, Wang KK, Povlishock JT. Biochemical, structural, and biomarker evidence for calpain-mediated cytoskeletal change after diffuse brain injury uncomplicated by contusion. J Neuropathol Exp Neurol. 2009; 68:241–249. [PubMed: 19225412]

McNamara KCS, Lisembee AM, Lifshitz J. The Whisker Nuisance Task Identifies a Late Onset, Persistent Sensory Sensitivity in Diffuse Brain-Injured Rats. J Neurotrauma. 2010 doi:10.1089/neu.2009.1237.

Passineau MJ, Zhao W, Busto R, Dietrich WD, Alonso O, Loor JY, Bramlett HM, Ginsberg MD. Chronic metabolic sequelae of traumatic brain injury: prolonged suppression of somatosensory activation. Am J Physiol Heart Circ Physiol. 2000; 279:H924–H931. [PubMed: 10993751]

Pons TP, Garraghty PE, Ommaya AK, Kaas JH, Taub E, Mishkin M. Massive cortical reorganization after sensory deafferentation in adult macaques. Science. 1991; 252:1857–1860. [PubMed: 1843843]

Povlishock JT, Becker DP, Cheng CL, Vaughan GW. Axonal change in minor head injury. J Neuropathol Exp Neurol. 1983; 42:225–242. [PubMed: 6188807]

Povlishock JT, Erb DE, Astruc J. Axonal response to traumatic brain injury: reactive axonal change, deafferentation, and neuroplasticity. J Neurotrauma. 1992; 9 Suppl 1:S189–S200. [PubMed: 1588608]

Povlishock JT, Katz DI. Update of neuropathology and neurological recovery after traumatic brain injury. J Head Trauma Rehabil. 2005; 20:76–94. [PubMed: 15668572]

Povlishock, JT.; Stone, JR. Traumatic axonal injury. In: Miller, LP.; Hayes, RL.; Newcomb, JK., editors. Head Trauma: Basic, Preclinical and Clinical Directions. Wiley; 2001. p. 281-302.

Singleton RH, Povlishock JT. Identification and characterization of heterogeneous neuronal injury and death in regions of diffuse brain injury: evidence for multiple independent injury phenotypes. J Neurosci. 2004; 24:3543–3553. [PubMed: 15071102]

Singleton RH, Zhu J, Stone JR, Povlishock JT. Traumatically induced axotomy adjacent to the soma does not result in acute neuronal death. J Neurosci. 2002; 22:791–802. [PubMed: 11826109]

Smith DH, Meaney DF, Shull WH. Diffuse axonal injury in head trauma. J Head Trauma Rehabil. 2003; 18:307–316. [PubMed: 16222127]

Stone JR, Walker SA, Povlishock JT. The visualization of a new class of traumatically injured axons through the use of a modified method of microwave antigen retrieval. Acta Neuropathol (Berl). 1999; 97:335–345. [PubMed: 10208272]

Thompson HJ, Lifshitz J, Marklund N, Grady MS, Graham DI, Hovda DA, McIntosh TK. Lateral fluid percussion brain injury: a 15-year review and evaluation. J Neurotrauma. 2005; 22:42–75. [PubMed: 15665602]

Thompson SN, Gibson TR, Thompson BM, Deng Y, Hall ED. Relationship of calpain-mediated proteolysis to the expression of axonal and synaptic plasticity markers following traumatic brain injury in mice. Exp Neurol. 2006; 201:253–265. [PubMed: 16814284]

Vaudano E, Campbell G, Anderson PN, Davies AP, Woolhead C, Schreyer DJ, Lieberman AR. The effects of a lesion or a peripheral nerve graft on GAP-43 upregulation in the adult rat brain: an in situ hybridization and immunocytochemical study. J Neurosci. 1995; 15:3594–3611. [PubMed: 7751932]

Waite, PME.; Tracey, DJ. Trigeminal Sensory System. In: Paxinos, G., editor. The Rat Nervous System. San Diego: Academic Press; 1995. p. 705-724.

Wieloch T, Nikolich K. Mechanisms of neural plasticity following brain injury. Curr Opin Neurobiol. 2006; 16:258–264. [PubMed: 16713245]
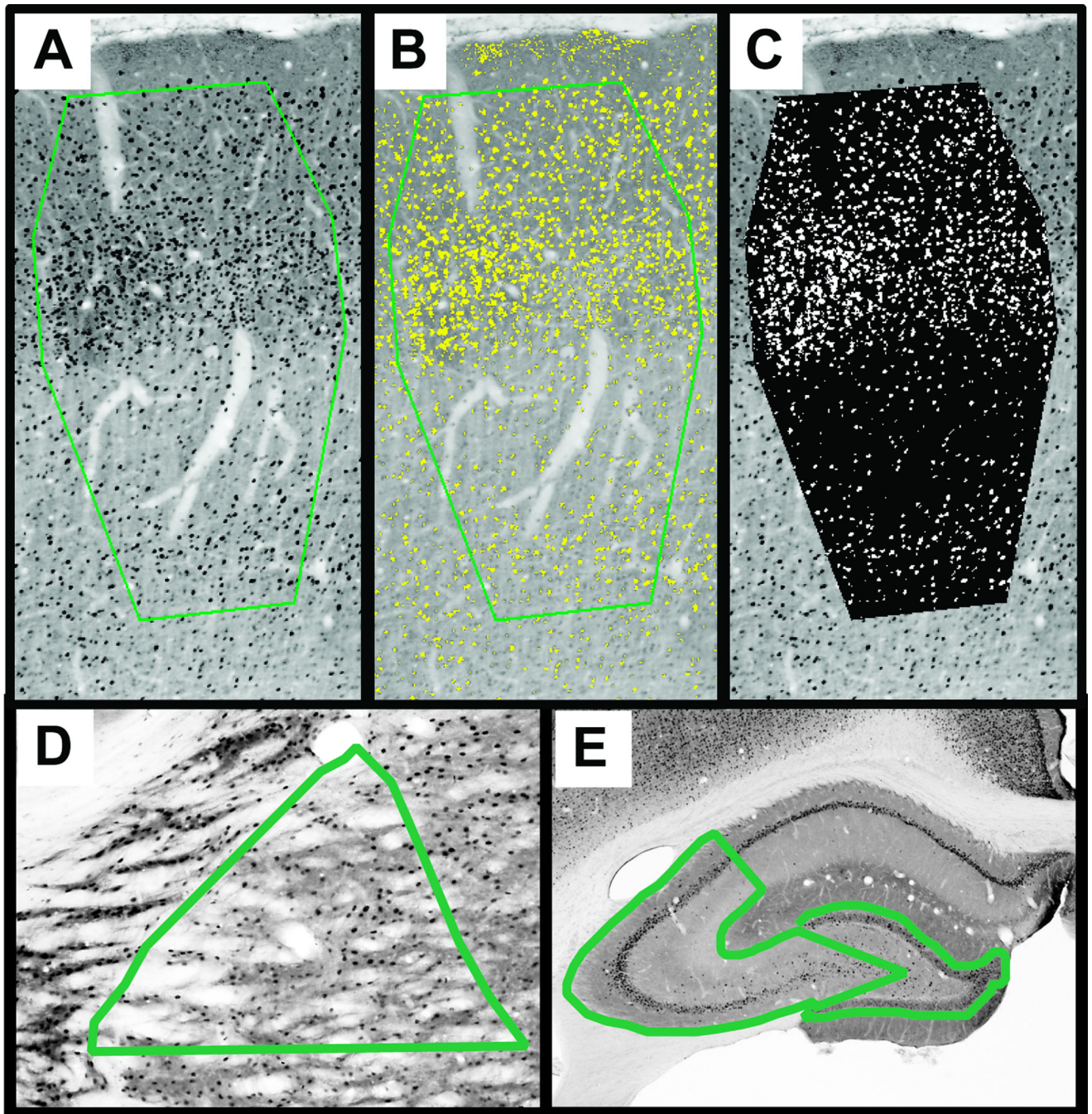
Figure 1.
A digital thresholding procedure was implemented to quantify neuronal activation in the primary somatosensory cortex, ventral posterior thalamus and hippocampus. (A) The region of interest (green border) is outlined to include cortical layers II through V and span the width of the layer IV barrels. Thresholds are adjusted to include immuno-positive staining (B, yellow). Pixels with positive staining are segmented from pixels in unstained tissue (C, white vs. black). The percentage of white pixels to black+white pixels provides the cFos labeling percentage presented in Figure 3. Measurements are replicated three times and averaged to obtain a value for each section. (D) Representative region of interest for the

ventral posterior thalamus. (E) Representative regions of interest for hippocampus area CA3 (left) and dentate gyrus (right).
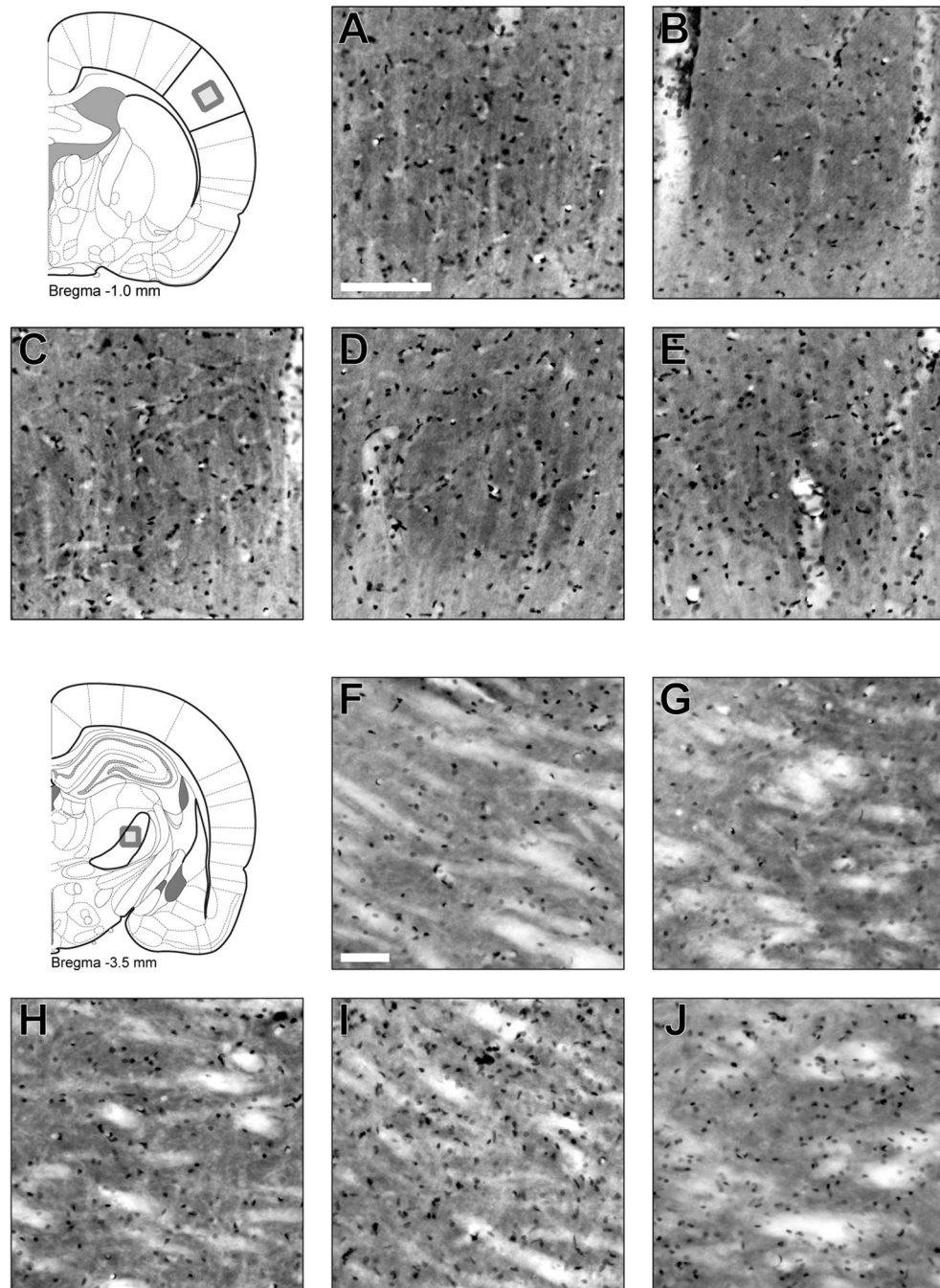
Figure 2.
Diffuse brain injury does not destroy the whisker barrel circuit. Coronal sections through primary somatosensory barrel cortex (A–E) and ventral posterior medial thalamus (F–J) were stained by cytochrome oxidase histochemistry and cresyl violet. Individual cortical barrels remain well defined and filled with nissl-positive cells in sham (A), 1 day (B), 2 day (C), 7 day (D) and 28 day (E) post-injury. In sections through the ventral posterior medial thalamus, similar staining is evident between sham (F), 1 day (G), 2 day (H), 7 day (I) and 28 day (J) post-injury. Scale bars are 100 µm.
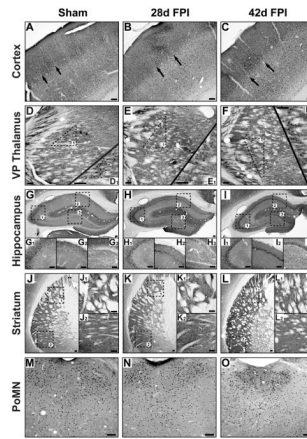
Figure 3.
In response to selective whisker stimulation, *cFos* immunohistochemistry (black dots) and cytochrome oxidase histochemistry (background stain) in uninjured sham (left column), 28d fluid percussion injured (FPI; middle column), and 42d FPI (right column) rats show predicted neuronal activation in the primary somatosensory cortex (A–C; arrows indicate edges of an activated barrel; −3.36 mm from bregma) and ventral posterior (VP) medial thalamus (D–F; −3.60 mm from bregma). Activated barreloids in the VPM were evident in all conditions (D_1, E_1, F_1). In sham brain, the activated neurons scattered in hippocampal area CA1 (G_2; −4.00 mm from bregma) are not found in area CA3 (G_1). In the injured brain, activated neurons are evident in area CA1 (H_2, I_2), but dwarfed by the activated neurons throughout area CA3 (H_1, I_1). In the dentate hilus, activated neurons are evident in the injured (H_3, I_3), but not uninjured tissue (G_3). Activated neurons throughout the dorsal (K_1, L_1; −2.00 mm from bregma) and ventral (K_2, L_2) striatum after brain injury contrasts the activated neurons selectively found in the dorsal striatum (J_1), but not ventral striatum (J_2) of sham animals. (M–O) Diffuse brain injury does not appear to effect neuronal activation in the posterior medial nucleus (PoMN; −4.00 mm from bregma) of the thalamus, a motor nucleus that controls whisking. All scale bars are 10 µm.
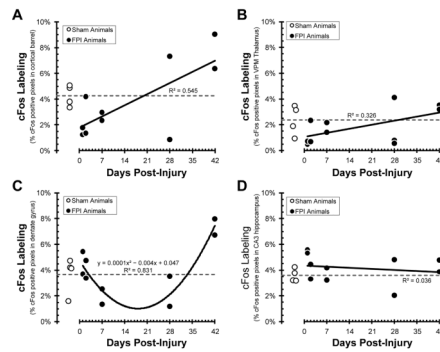
Figure 4.
Pixel quantification of cFos labeling of uninjured (open circles) and fluid percussion injured (FPI) animals (closed circles) over a 42 day post-injury time course (see methods for details). The open circles and horizontal dashed line indicate activation following whisker stimulation in individual uninjured sham animals and the group average, respectively. (A) In the somatosensory barrel fields, over the first week post-injury, fewer cortical barrel pixels were activated by whisker stimulation. At 28–42 days post-injury, cFos labeling exceeds sham levels. The positive correlation between cFos labeling and time post-injury (r^2=0.545) indicates a greater extent of neuronal activation following diffuse brain injury. (B) In the ventral posterior thalamus barreloids, over the first week post-injury, fewer pixels were activated by whisker stimulation. At 28–42 days post-injury, cFos labeling returns to sham levels. (C) In the hippocampus dentate gyrus, cFos labeling declined over the first week post-injury, remained depressed through 28 days, and exceeded sham values by 42 days post-injury. The data fit a U-shaped, second-order polynomial correlation between time post-injury and cFos labeling (r^2= 0.831). (D) In the hippocampus area CA3, cFos labeling remained unchanged from sham values over the 42 day time course.
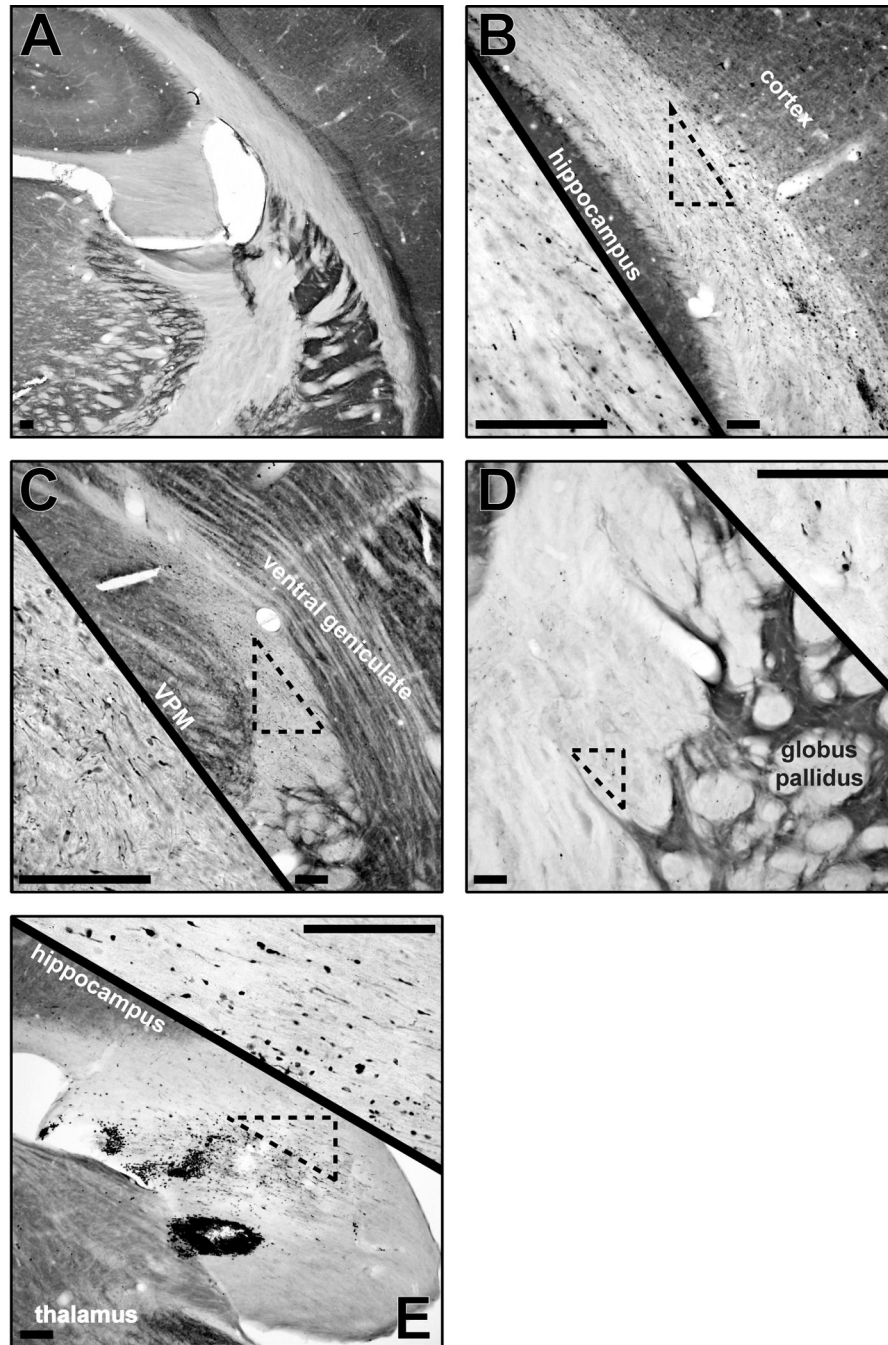
Figure 5.
Cytochrome oxidase histochemistry (background stain) with amyloid precursor protein (APP) immunohistochemistry (black) in uninjured sham (A; −3.24 mm from bregma) and 2d brain-injured (B–E) rats demonstrate the extent of axonal pathology across the subcortical white matter (B; −4.56 mm from bregma), superior thalamic radiation (C; −4.56 mm from bregma), internal capsule (D; −1.56 mm from bregma) and fimbria of the hippocampus (E; −3.48 mm from bregma). Axonal injury is identified by APP-positive immunoreactivity and swollen axonal segments or terminal bulbs. Scattered pathology is evident in the low magnification images and the high magnification insets. All scale bars are 10 μm.
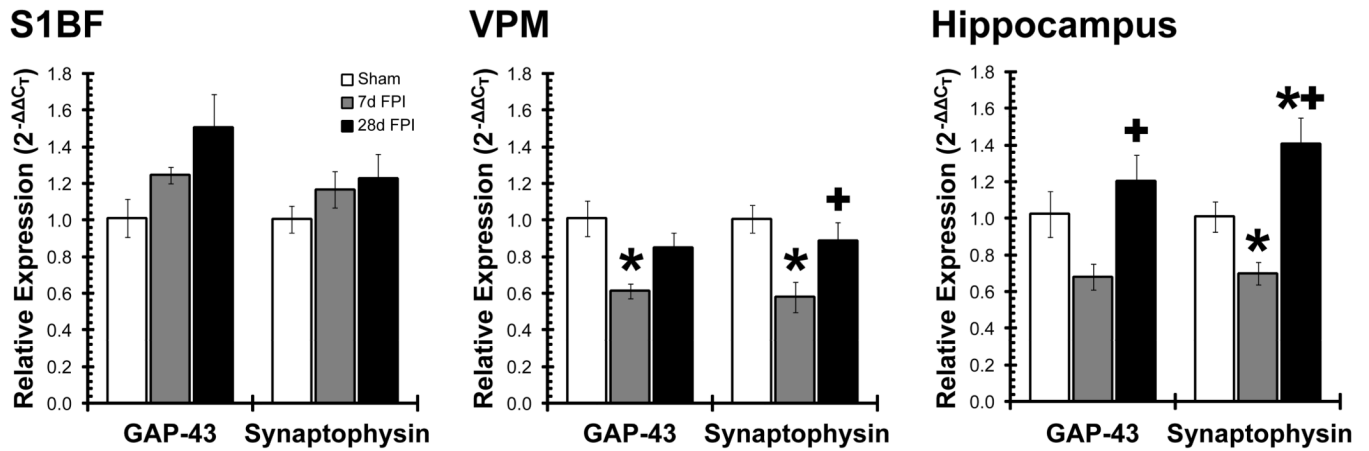
Figure 6.
Gene expression indicates a neuroplastic response after diffuse brain injury. From sham, 7d and 28d fluid percussion brain-injured (FPI) animals, mRNA was isolated from the somatosensory cortex (S1BF), ventral posterior medial thalamus (VPM) and hippocampus. The relative expression of sprouting genes (GAP-43, synaptophysin) was quantified using real-time quantitative PCR. In S1BF, plasticity markers continually increased, whereas plasticity markers in VPM and hippocampus initially decreased and then returned to or above uninjured levels. *, $p < 0.05$ vs. sham; +, $p < 0.05$ vs 7d FPI.